The Iranian Journal of Mechanical Engineering Transactions of ISME
Journal homepage: https://jmee.isme.ir/
Vol. 25, No. 2, 2024, pp. 63-77

Research Paper

DOI: https://doi.org/10.30506/jmee.2024.2016270.1334

Implementation of Local Chemiluminescence Method on a Premixed Laminar Propane/Air Flame

Anahita Reyhani[*]
Ph.D. Candidate

Azadeh Kebriaee[†]
Assistant Professor

In this work, the local chemiluminescent intensities of OH and CH* of a premixed laminar Propane/air bunsen burner flame have been measured. A multi-color integrated Cassegrain receiving optics (MICRO) is developed. The design of the optical system is optimized to minimize optical aberrations, especially spherical aberration. The effective light collection volume of the system is estimated to be a cylinder with 58 micrometers in diameter and 3.4 millimeters in depth. The Temporal resolution of the data acquisition system in this work is 2 microseconds. The effect of the equivalence ratio on the OH*/CH* signal is investigated and the calibration curve is extracted between the equivalence ratio and the OH*/CH* signal in a certain range of equivalence ratios for Propane/air combustion.*

Keywords: Optical measurement, Lens design, Chemiluminescence method, Premixed combustion

1 Introduction

Flame chemiluminescence is an optical signature of the combustion process and is an interesting alternative for combustion diagnostics [1]. Researchers have shown that there are relationships between the chemiluminescent emission of combustion radicals and combustion parameters.
For Instance, Clark [2] showed that there is a correlation between the chemiluminescent emission of combustion radicals and the equivalence ratio. Najm et al. rate [3] studied the correlation between heat release rate and the chemiluminescent emission of combustion radicals. Higgins et al. [4] studied the correlation between total mass consumption and the chemiluminescent emission of combustion radicals. Also, many other researches have been conducted that have studied the correlation between the chemiluminescent emission of combustion radicals and other combustion parameters.

[*]Ph.D. Candidate, Department of Aerospace Engineering, Sharif University of Technology, Tehran, Iran, anahitareyhani76@gmail.com
[†]Corresponding author, Assistant Professor, Department of Aerospace Engineering, Sharif University of Technology, Tehran, Iran, kebriaee@sharif.ir

Received: 2023/11/22, Accepted: 2024/06/30

Gaydon et al. [5-7] did some spectroscopic studies on hydrocarbon flames and investigated the relationship between chemiluminescent emissions and combustion parameters. Higgins et al. [4] studied the effect of equivalence ratio and the pressure on the chemiluminescent emission of OH* from CH4/air combustion. They showed that the measurement of the chemiluminescent emissions of the combustion can be used to monitor the combustion process to reduce NOx emission.

In recent years, some experimental studies have been done on local chemiluminescence. Akamatsu et al. [8] have developed a high-luminosity-light-collection system for highly spatial detection of chemiluminescence of radical species in flames based upon a Cassegrain-type configuration. Other researchers have used the Cassegrain-based optical system to investigate the chemiluminescent emissions of combustion radicals. Ikeda et al. [9] used the Cassegrain-based optical system to measure spatially resolved chemiluminescence spectra of high-pressure premixed methane/air flame. Kojima et al. [1] made a study of the spatial intensity profiles of combustion radicals chemiluminescence in atmospheric-pressure laminar CH4-air premixed flames over a range of equivalence ratios by the use of Cassegrain-based optics. Hardalupas et al. [10] used a Cassegrain-based chemiluminescence sensor for measurements in gas turbine combustors and showed that this sensor can be used to monitor the degree of premixedness of reacting fuel and air in industrial gas turbine combustors and show that CH* and OH* are suitable indicators for heat release rate.

Hardalupas et al. [11] theoretically and experimentally measured the spatial resolution of a chemiluminescence sensor for local heat-release rate and equivalence ratio in a model gas turbine combustor and used the Cassegrain-based optical system to study combustion reaction zone, heat-release rate, and local equivalence ratio in a bunsen burner flame and a combustion chamber with a swirl-stabilizes flame.

In this report, the experimental setup used to implement local chemiluminescence on a premixed laminar Propane/air bunsen burner flame is introduced and the design process of the Cassegrain-based optical system is explained. The result of this work is the extraction of the calibration curve between the equivalence ratio and the OH*/CH* signal.

2 Methodology

In the combustion process, some excited radicals will be formed. When the excited species returns to a lower energy level, it emits electromagnetic waves in the form of light. This process is shown in Eq. (1). [12] In this equation, h is the Plank's constant and f is the frequency of the chemiluminescence.

$$AB^{*} \rightarrow AB + hf \tag{1}$$

In Hydrocarbon flames, chemiluminescent emissions are from three major radicals including OH^{*}, CH^{*}, and $C_2{}^{*}$. These major radicals are along with $CO_2{}^{*}$ background radiation [13]. Each Combustion radical on the way to return to a lower energy level, emits electromagnetic waves in a unique range that can be the indicator of this excited radial in the combustion process.

The major radicals of the hydrocarbon flame combustion, the reaction forming them, and the main band location of their electromagnetic emission in the spectrum of electromagnetic waves are shown in Table 1. Also, the emission spectrum of the combustion radicals for a hydrocarbon flame is shown in Figure (1). In the present research, the fact that OH^{*} radical and CH^{*} radical have electromagnetic emissions in a certain range of wavelength has been used to develop an experimental test setup to measure the intensity of the emissions of these radicals.

Table 1 Combustion radical in hydrocarbon flames, their main formation reaction and main band location [14]

Species	Main formation raction in hydrocarbon flame	Main band location (nm)
OH^*	$CH + O_2 \rightarrow CO + OH^*$	283, 306-315
OH^*	$C_2 + OH \rightarrow CO + CH^*$ $C_2H + O \rightarrow CO + CH^*$	390, 431
C_2^*	$CH_2 + C \rightarrow H_2 + C_2^*$ $CH + C \rightarrow H + C_2^*$	469-473, 510-516
CO_2^*	$CO + O + M \rightarrow CO_2^* + M$	~300-500

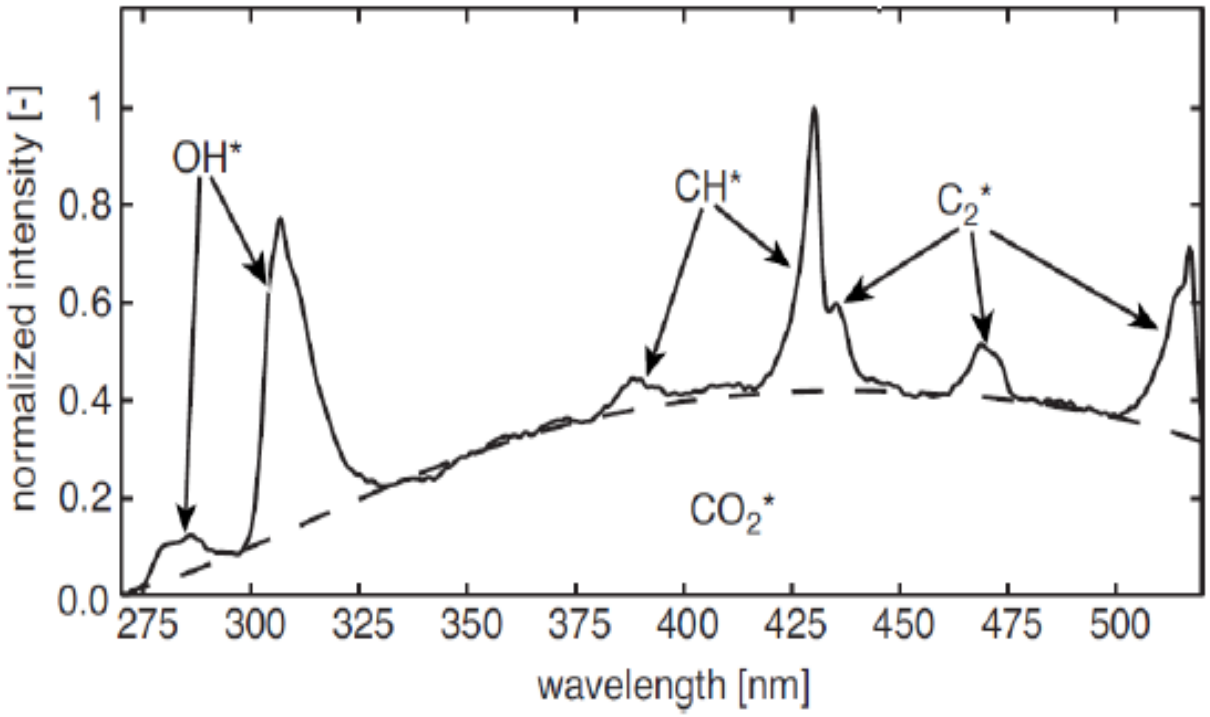

Figure 1 Emission spectrum for a hydrocarbon flame [15]

3 Experimental apparatus

The experiments were carried out using a bunsen burner with a laminar, premixed Propane/air flame. The flow rate of air and fuel were adjustable to achieve different fuel flow rates and equivalence ratios. The flame setup is shown in Figure (2). To achieve high spatial resolution, a multi-color integrated Cassegrain receiving optics (MICRO) was developed. MICRO is a light-collecting probe based on Cassegrain optics that are commonly used in astronomical reflecting telescopes having an infinite conjugate ratio [8].

The probe consists of a concave mirror with a hole in the center and a convex mirror. The concave mirror that is the primary mirror is 150 millimeters in diameter and has a radius of curvature of 300 millimeters. The convex mirror that is the secondary mirror is 50 millimeters in diameter and has a radius of curvature of 200 millimeters. The rays from the effective control volume first hit the concave mirror and are reflected then they hit the convex mirror and are reflected and pass through the hole that is in the center of the concave mirror and are focused in a circle where the head of the optical fiber is put there. This circle is called the circle of least confusion where the bundle of rays emitted from the control volume center is focused onto the smallest area possible [8].

The Cassegrain optics consists only of mirrors thus no chromatic aberration occurs and the spherical aberration is canceled out by using an optimized combination of concave and convex mirrors, which have opposite light-reflection effects [8].
Zemax program was used in different steps of the optical system design process. The initial design of the Cassegrain-based optical system was done using the Gaussian lens equation of the paraxial approximation [16] and in the next step, optimization was done using Zemax program.
The effect of the diameters of the mirrors on the size of the effective control volume was examined with the use of the Zemax program in the non-sequential mode and placing a detector in the circle of least confusion. It was concluded that the diameters of the mirrors do not affect the size of the effective control volume. It only affects the power of light that is collected. The results are shown in Table 2. It is clear that the larger the aperture of the optical system gets, the more light power is recovered by the system.

As it was shown, a larger aperture choice that leads to the need to use larger diameters for the primary and the secondary mirror makes the optical system more expensive and also heavy and bulky. The diameters of the mirrors were chosen from previous works [8] to be sure that enough light power is provided.

Figure 2 Flame Setup

Table 2 Effect of the aperture size on the performance of the optical system

Optical aperture (mm)	Primary mirror diameter (mm)	Secondary mirror diameter (mm)	Input light power (W)	Output light power (W)	Light power recovered (%)
100	99.084	31.506	500	96.35	10.08
150	146.954	46.996	500	124.85	24.97
200	192.920	62.184	500	206.30	41.26
250	236.508	77.21	500	326.56	65.31

The optical system should be at a sufficient distance from the flame to avoid thermal expansions and this is one of the constraints governing the design process. The effective focal length of the system which is called the working distance was set at 300 millimeters. This length is sufficiently longer than the flame height. In the optimization process, this length became 296.208 millimeters.

The design parameters were the radius of curvature for each mirror, the distance between the mirrors, and the place of the circle of least confusion. Cassegrain optics governing equations which are the Gaussian lens equation of the paraxial approximation were used to make a suitable first guess for design parameters [16]. After that, some trial and error were done in the Zemax program to make the first guess more reasonable. the Gaussian lens equation of the paraxial approximation that has been used in the design process of the Cassegrain optical system is shown in Eq. (2) [16]. In this equation, f is the focal length of the optical surface and S is the distance between the object or the Image and the optical surface. A positive value of S indicates a real object or image and a negative value of S indicates a virtual object or image. The other equation that has been used in the primary design process of the Cassegrain optical system, is Eq. (3) which shows that in a spherical optical surface, the focal length has half of the value of the radius of curvature of the optical surface.

$$\frac{1}{f_0} = \frac{1}{S_1} + \frac{1}{S_2} \tag{2}$$

$$f = \frac{R}{2} \tag{3}$$

At last, the radius of curvature of the mirrors was fixed and the distance between the mirrors and the place of the circle of least confusion was optimized in the Zemax program with the use of the ray-tracing method and definition of a proper merit function that shows the quality of the performance of the optical system. The mathematical definition of the merit function is shown in Eq. (4). In this equation d is a deviation from the ideal system and W is the weight of this deviation. As it is clear, the value of the merit function for an ideal optical system is equal to zero [17].

$$MF = \sum_{i=1}^{i=n} W_i d_i \tag{4}$$

The goal of this design problem is to focus the light that is collected from the effective control volume in the smallest circle possible and have an image free of any kind of optical aberration.

To reach that goal the Zemax program minimizes the RMS of the spot radius from the centroid to optimize the design thus the design parameters were chosen so that the optical system can focus the light collected from the effective control volume in the smallest possible circle. The mathematical definition for RMS is shown in Eq. (5). The final design after the optimization process is shown in Figure (3).

$$\mathrm{RMS} = \sqrt{\frac{\sum_{i=1}^{i=n}[(x_i - x_c)^2 + (y_i - y_c)^2]}{n}} \tag{5}$$

The spot diagram of the Cassegrain-based optical system on the Image plane is shown in Figure (4). It shows that the radius of the least confusion circle is 0.349 micrometers. The point spread function (PSF) was drawn in the polychromatic logarithmic FFT mode to check the performance of the optical system. The polychromatic logarithmic FFT PSF is shown in Figure (5). It shows that the system has an acceptable performance.

The seidel aberration coefficients diagram for various kinds of aberrations of the system is shown in Figure (6). This figure shows that how the spherical aberrations of the mirrors cancel out each other. Also, it is shown that the optimized system is free of any kind of optical aberration and the optimization process has been successful. The effective control volume was measured in the Zemax program. It was estimated to be a cylinder with 58 micrometers in diameter and 3.4 millimeters in depth.

The head of an optical fiber with a numerical aperture of 0.22 and an acceptance angle of 25.4 degrees and a core diameter of 100 micrometers was placed at the circle of least confusion. In the mechanical design, the place of the optical fiber head and the primary mirror were fixed but the place of the secondary mirror was changeable thus the errors in the radius of curvature of the mirrors that may occur during the manufacturing process can be compensated with the change of the distance between the mirrors and the distance between the optical system and the flame. A lead screw was used to provide movement ability for the secondary mirror.

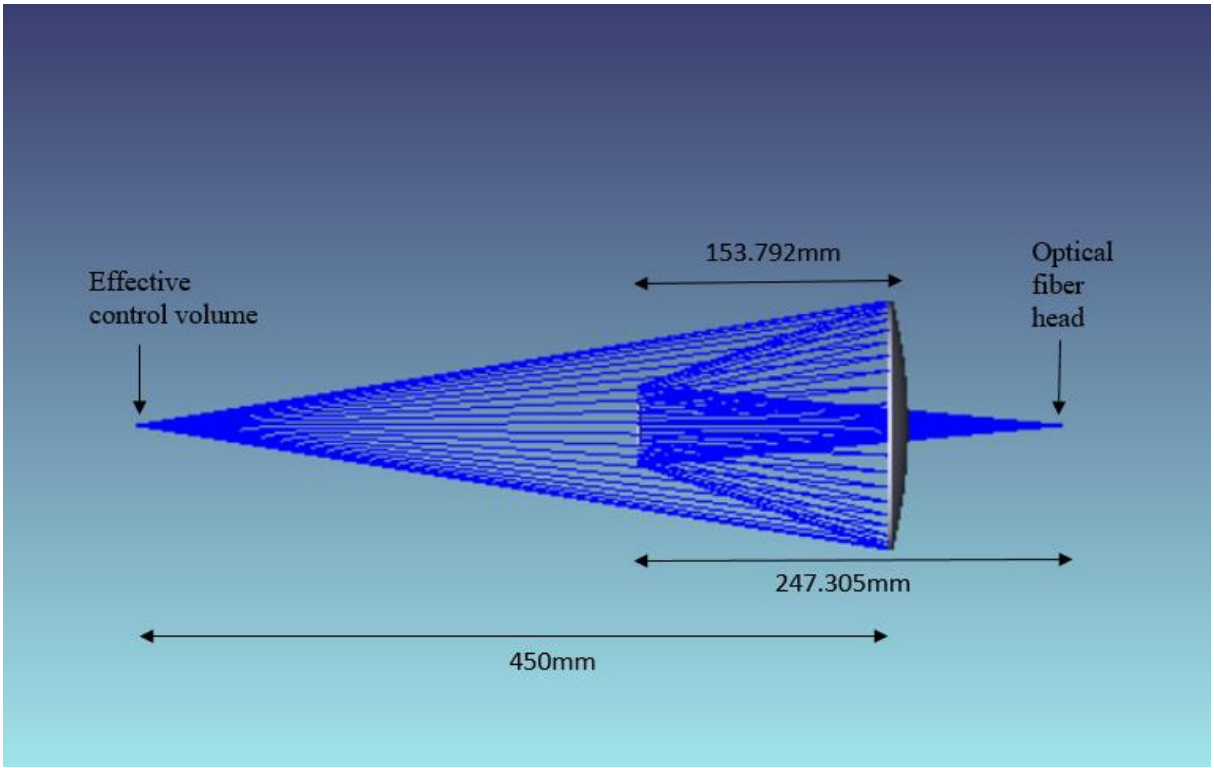

Figure 3 Schematic of the designed Cassegrain-based optical system

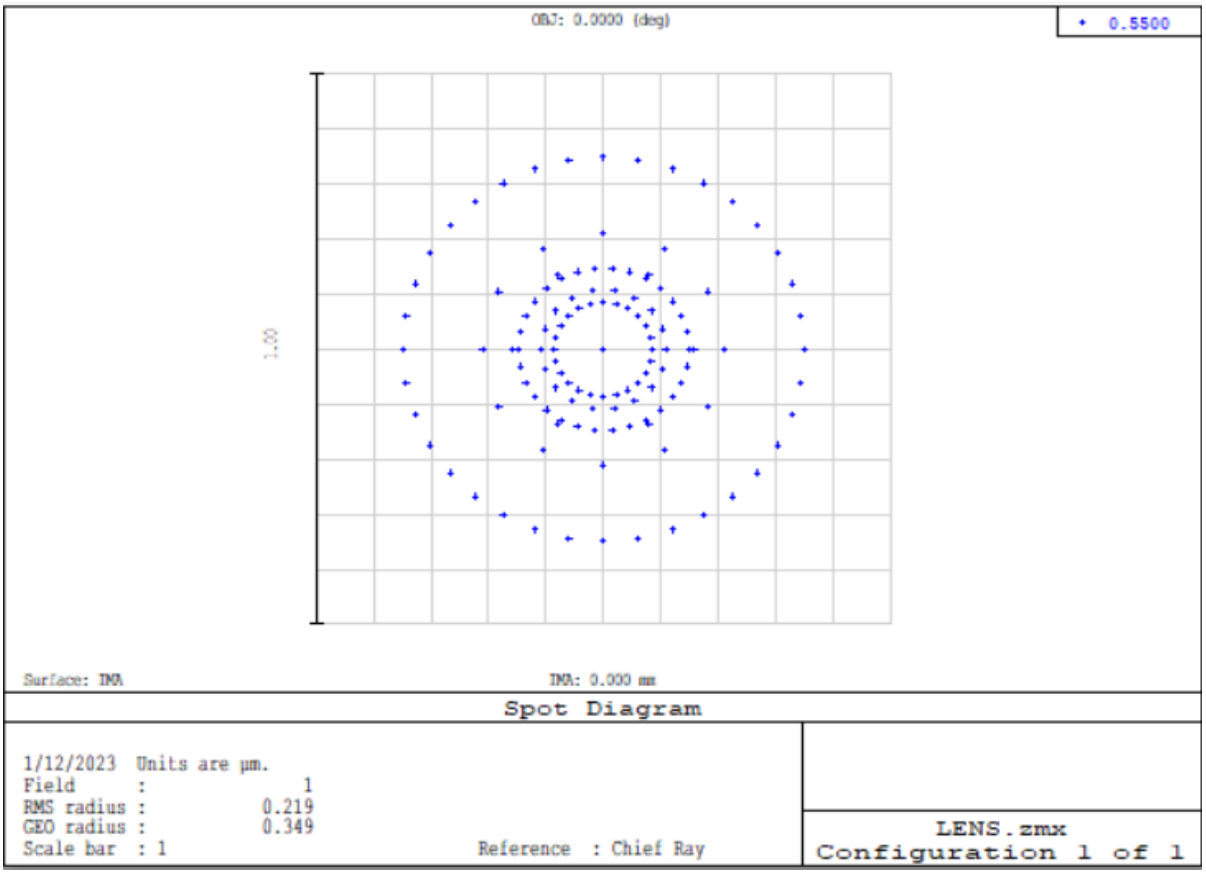

Figure 4 Spot diagram of the Cassegrain-based optical system

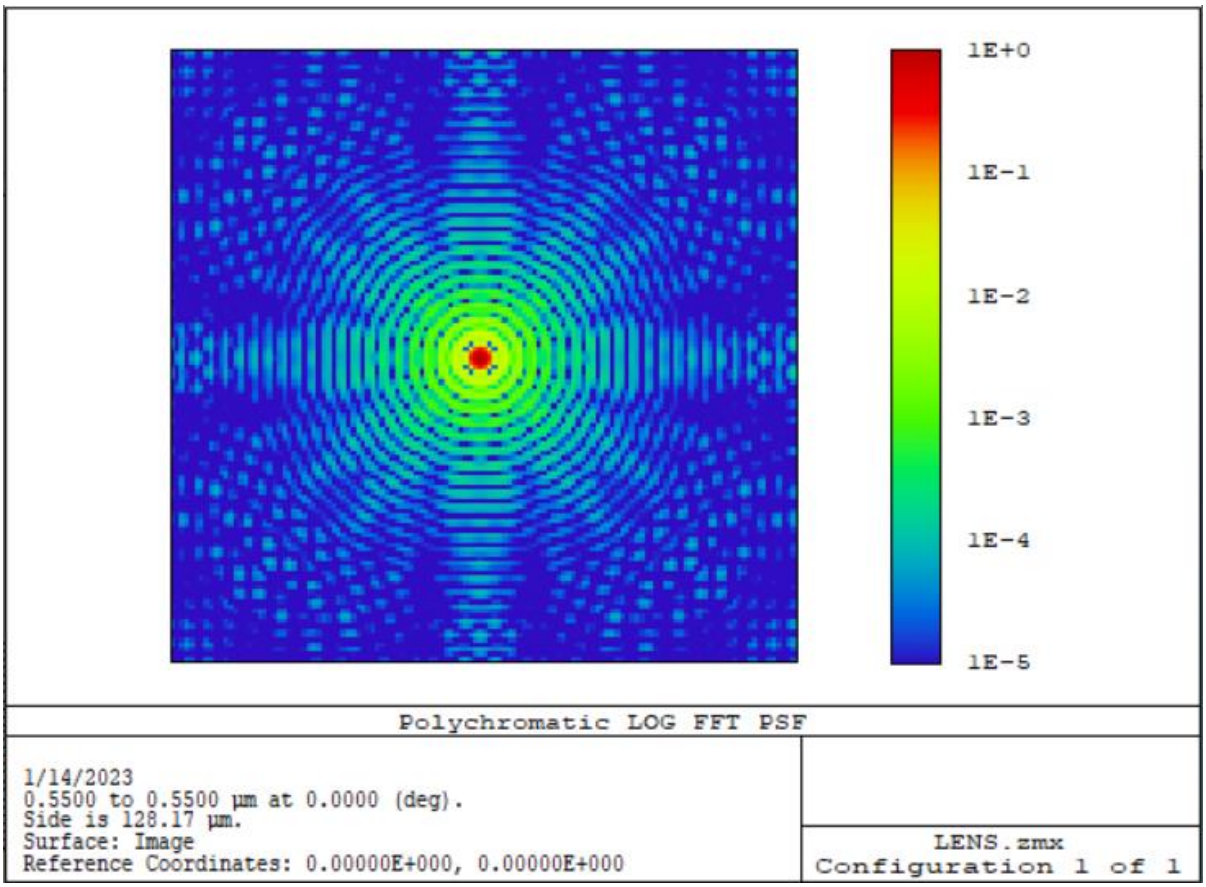

Figure 5 Polychromatic logarithmic FFT PSF of the Cassegrain-based optical system

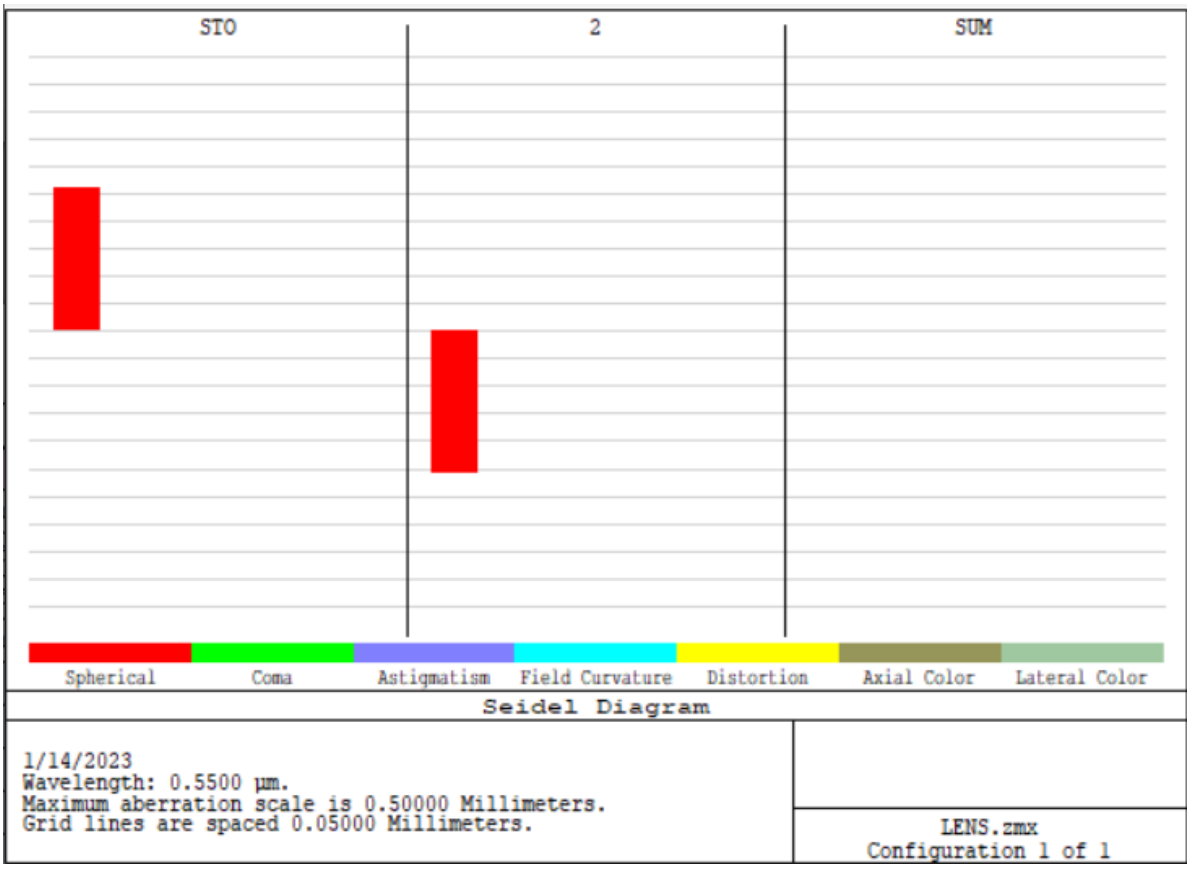

Figure 6 Seidel diagram of aberrations of the Cassegrain-based optical system

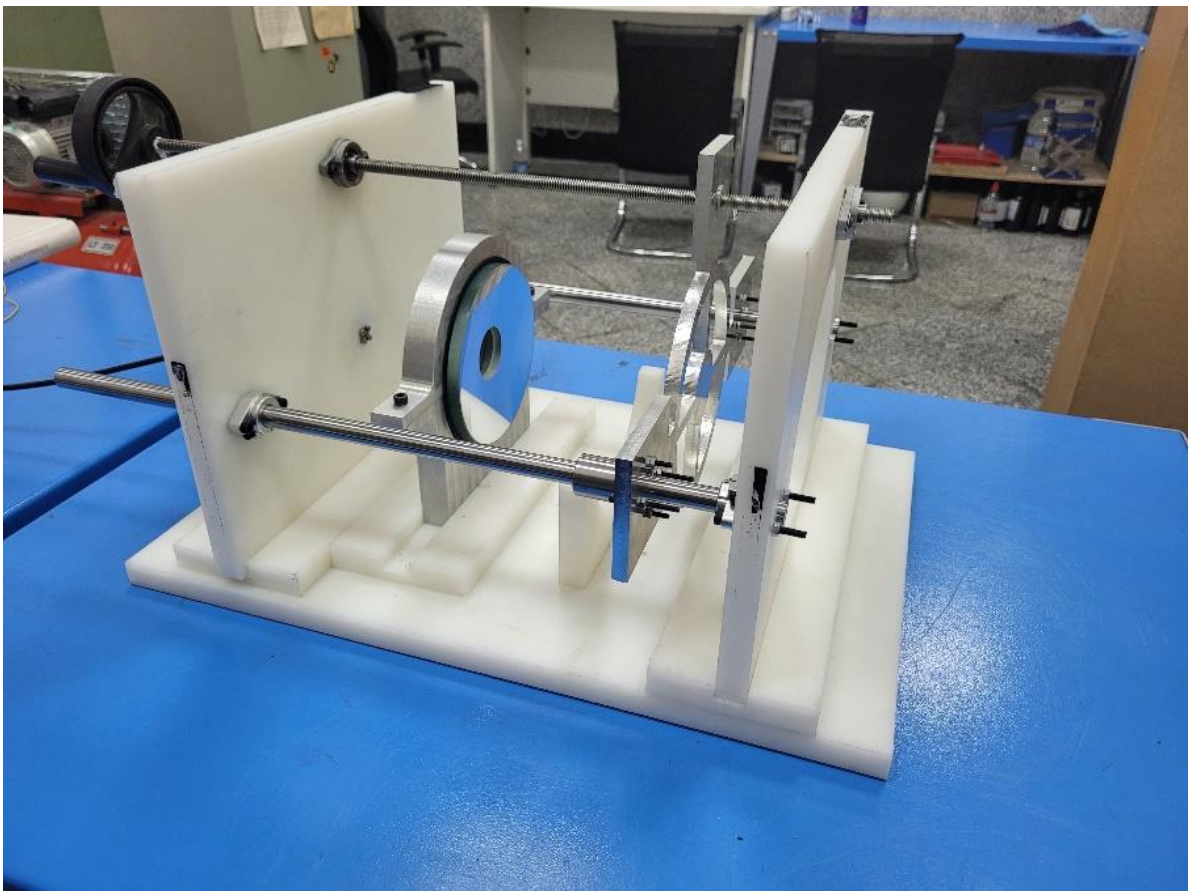

Figure 7 Cassegrain-based optical system

Various amounts of manufacturing-related errors in the radius of curvature of the mirrors were examined in the Zemax program, the optimization process was done for these new radiuses of curvatures, and the optimum distance between the mirrors and between the optical system and the flame was calculated.
The mechanical design was shown to be usable when the manufacturing tolerance of the radius of curvature of the mirrors be 10 micrometers and the design is reliable and the errors in the radius of curvatures of the mirrors can be compensated with the changing of the distance between mirrors and the working distance of the Cassegrain-based optical system.
Using Zemax program it was also shown that if there is a need to change the working distance of the system due to the flame condition, it is possible to use the developed Cassegrain-based optical system in a different working distance by changing the distance between the mirrors. The developed Cassegrain-based optical system is shown in Figure (7).
The optical fiber was connected to the detection block at its end. In the detection block first, light passes through a collimating lens to achieve a collimated bundle of light from the lens. The collimated light rays hit a dichroic filter. The dichroic filter separates the light rays based on the wavelength. It transmits light rays at the wavelength of 310.4 nanometers which is the wavelength at OH* emission occurs [10] and reflects light rays at the wavelength of 430.5 nanometers which is the wavelength at OH* emission occurs [10].
The separated light rays pass through bandpass filters with proper wavelength ranges. The bandpass filters have 10 nanometers passbands with center wavelengths equal to the wanted wavelengths. After passing through the filters, each bundle of lights hits a photomultiplier tube (PMT). PMTs were used as detectors. PMTs convert light to electrical current and to measure the intensity of the light in each wavelength, the measurement of the output current of each PMT was done. The output current of the PMTs was converted to voltage and become recorded. The filtering and detection unit is shown in Figure (8).
The detection block was connected to a data acquisition unit. Th rate of data acquisition was 500,000 samples per second which is equal to the temporal resolution of 2 microseconds. A Matlab code was developed to apply a low pass filter to the recorded data and analyze the results.

4 Results

To obtain the results and extract the calibration curve for the experimental setup and the fuel, the Cassegrain optical lens is focused on a point near the boundary of the flame. The point is approximately shown in Figure (9). The output of the detection unit of this research is voltage pulse. An example of the output of the detection unit is shown in Figure (10). To exclude the noise from the results and find the intensity of the emission of each studied radical, a lowpass filter was applied to the voltage pulses and with considering a threshold, the output pulses were counted. The number of pulses is proportional to the intensity of the light hitting the photomultiplier tubes. An example of the pulse counting is shown in Figure (11).
The effect of the equivalence ratio on the OH*/CH* signal was investigated and the calibration curve was extracted between the equivalence ratio and the OH*/CH* signal. The calibration curve is shown in Figure 12. It was shown that the OH*/CH* signal is a function of the equivalence ratio and the optical system for the tested propane/air flame. Thus, the curve that is extracted between the OH*/CH* signal and the equivalence ratio is the calibration curve for the optical system for every Propane/air flame.
With this calibration curve, using the developed Cassegrain-based optical system and optical filtering and detection system, and the data acquisition system, the equivalence ratio can be obtained locally for every propane/air flame with high temporal and spatial resolution. It should be mentioned that in the present research, the background emission of CO_2^* radical is not measured and has not been excluded from the results.

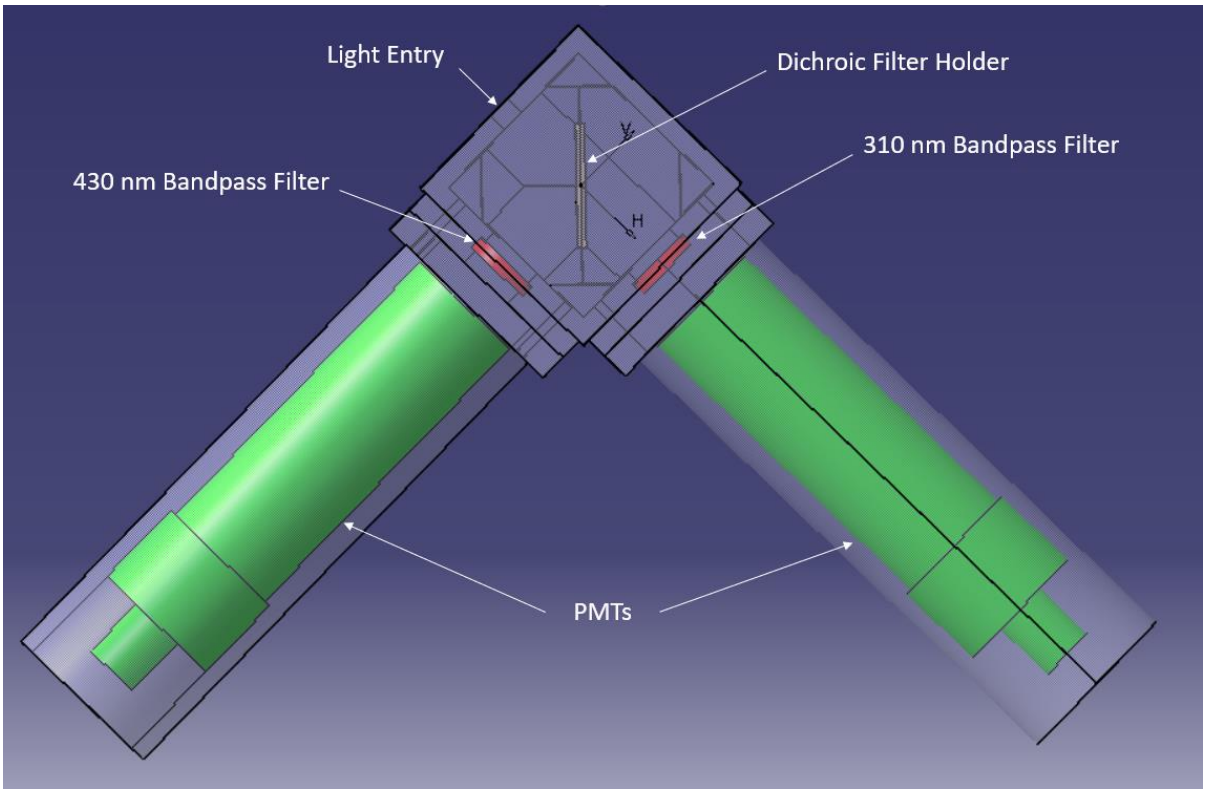

Figure 8 Filtering and detection unit

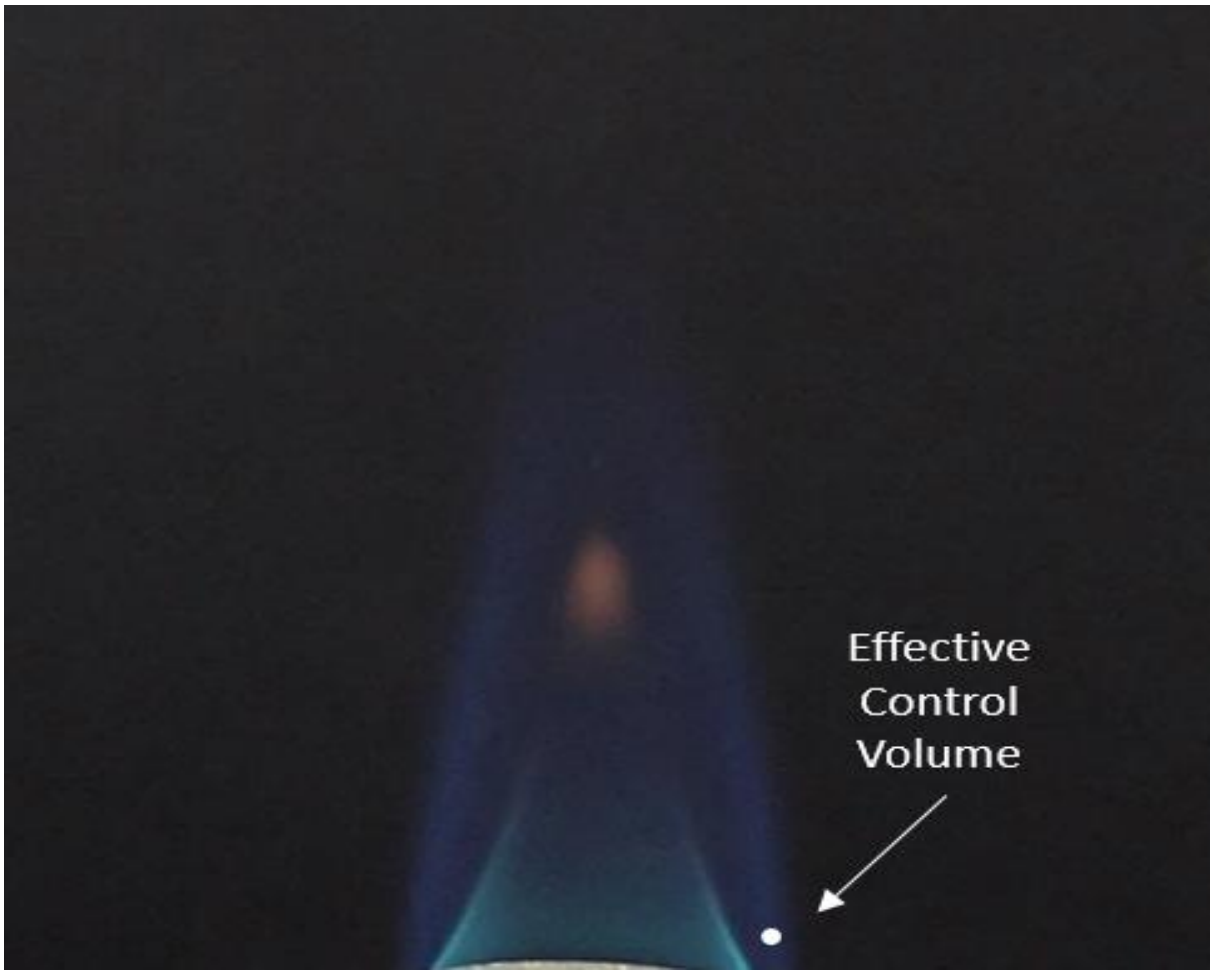

Figure 9 Approximate place of the effective control volume to collect light

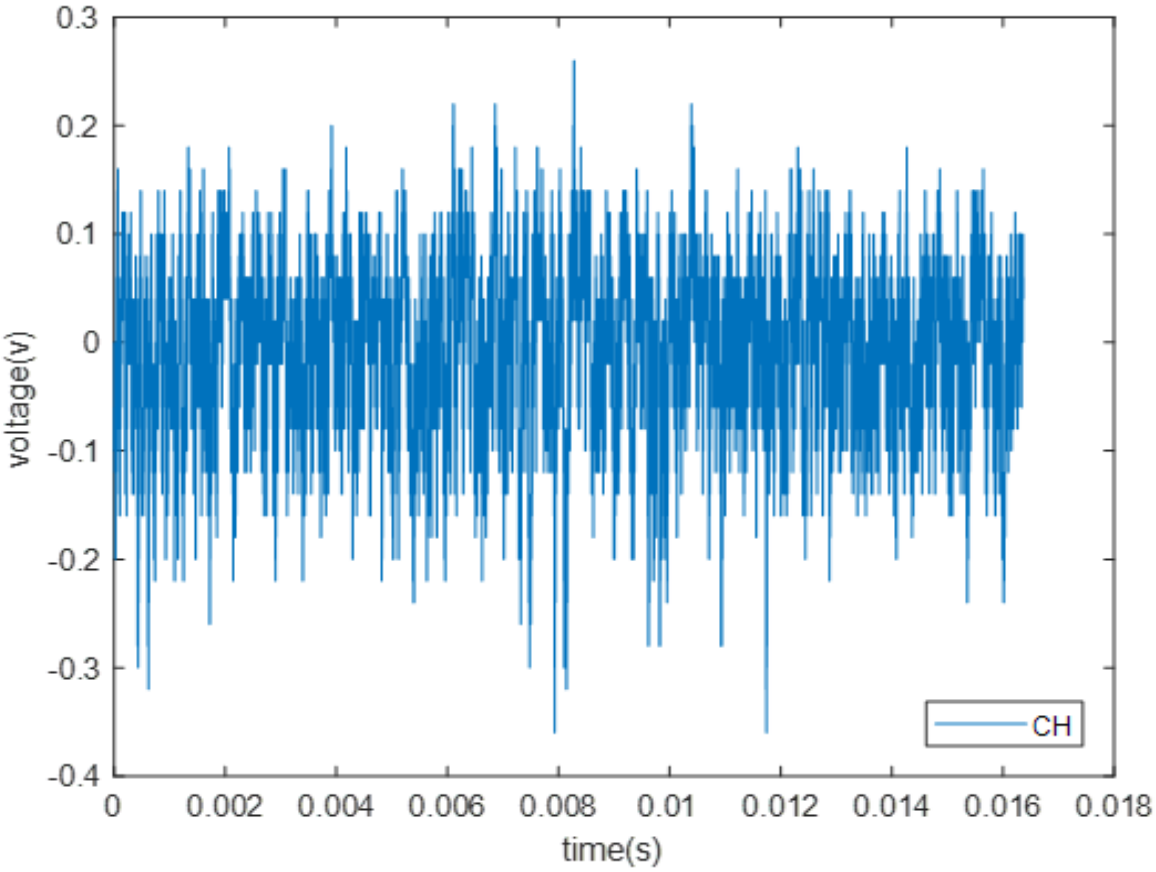

Figure 10 Sample voltage pulse output of the detection system

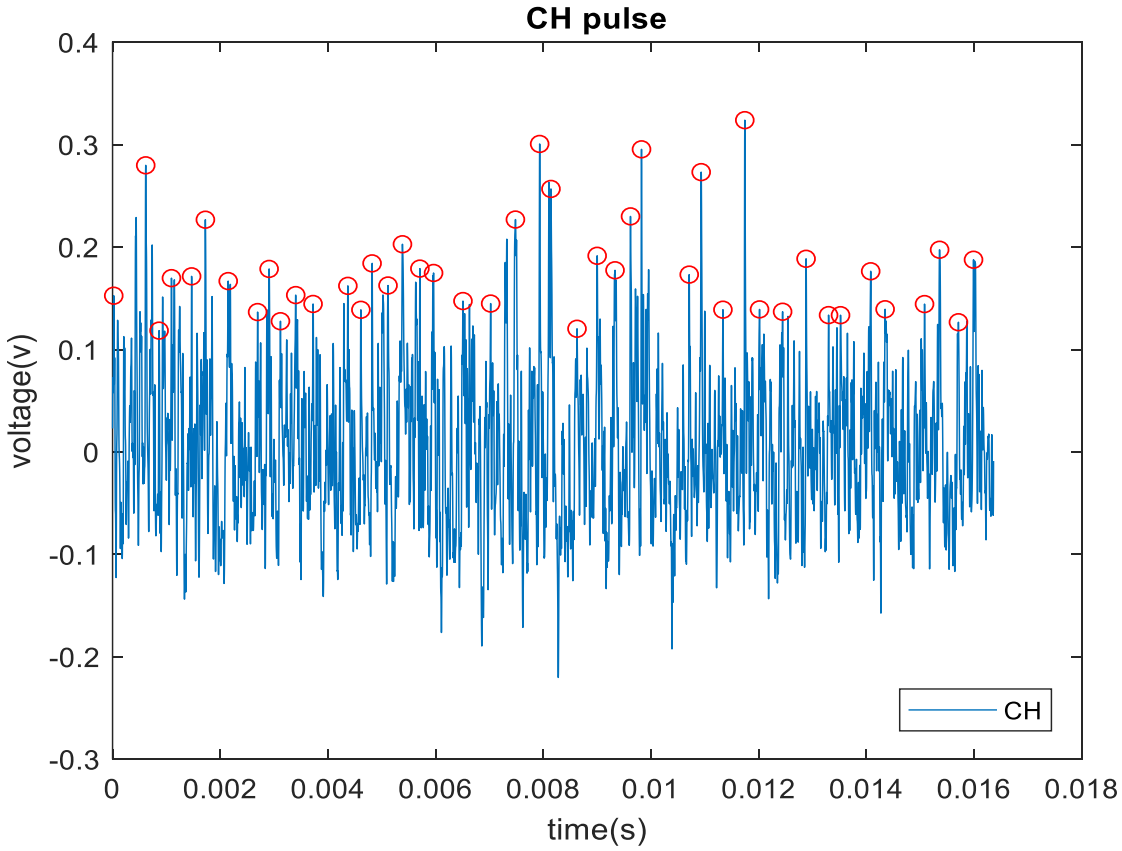

Figure 11 Sample pulse counting

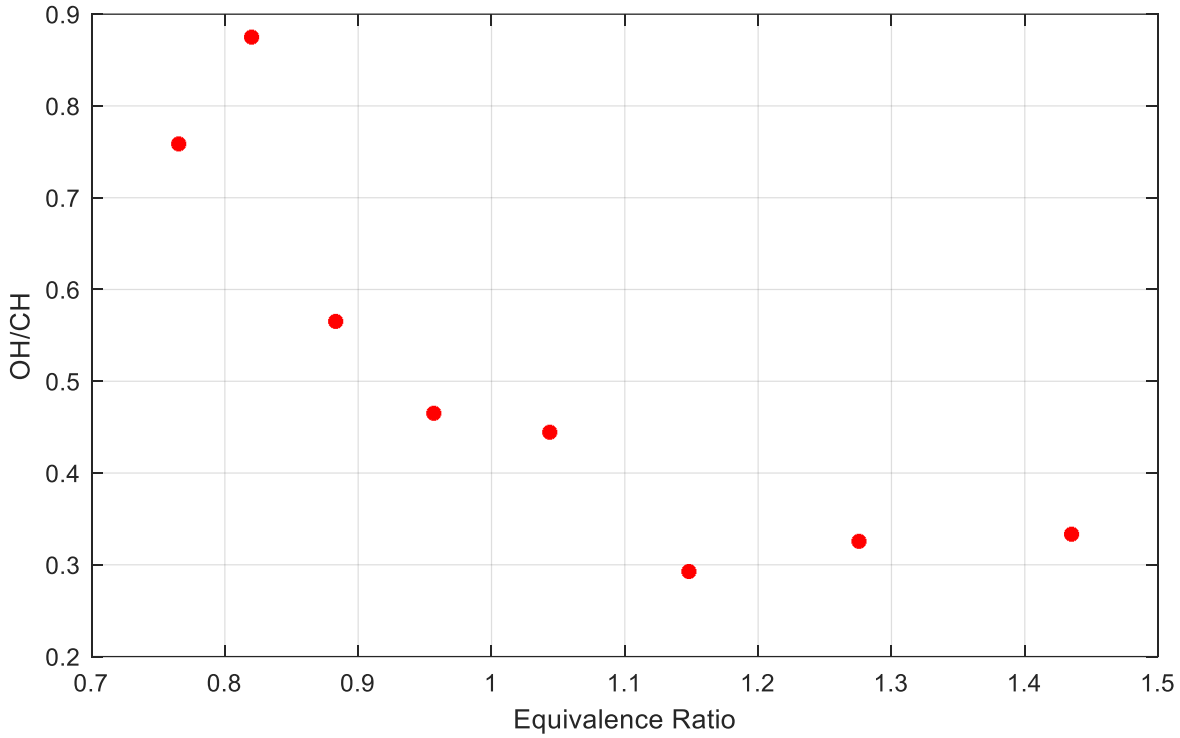

Figure 12 Calibration curve for propane/air flame

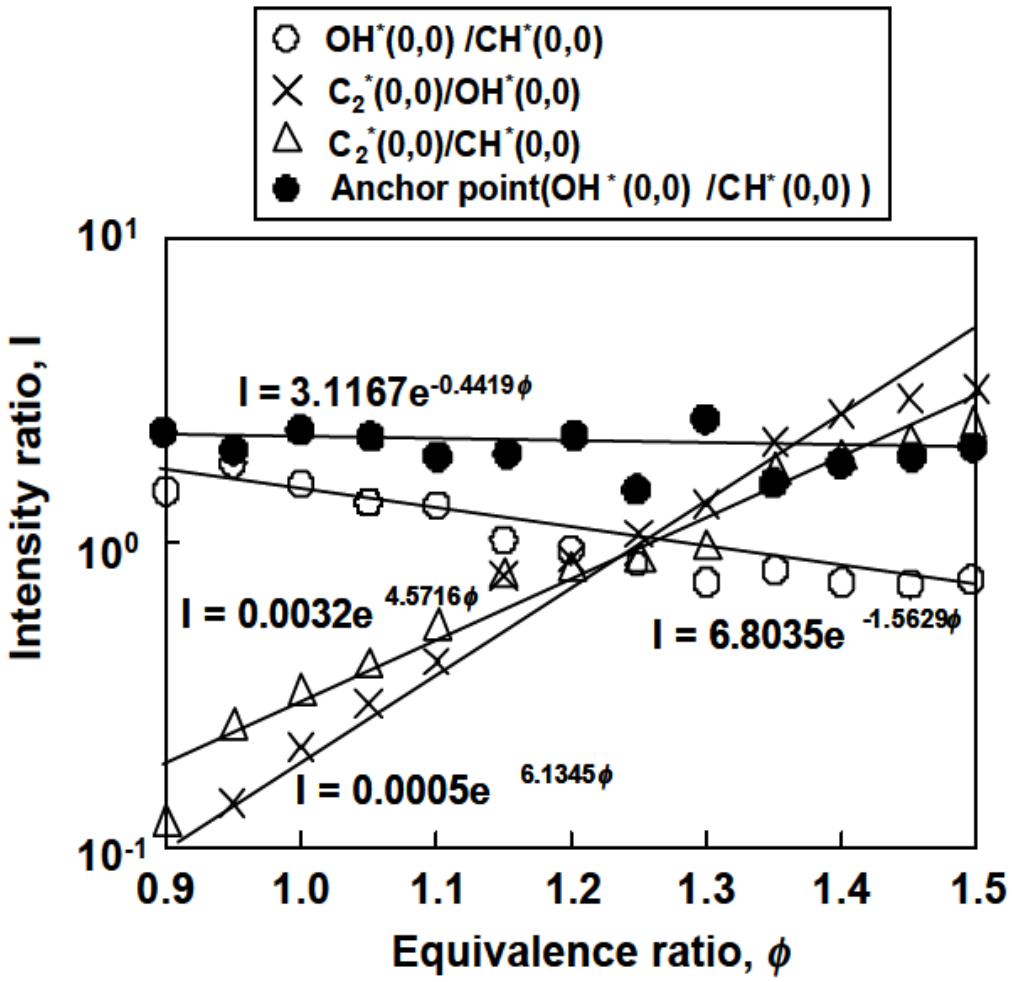

Figure 13 Calibration curve for propane/air flame by Ikeda et.al [18]

To validate the calibration curve that has been extracted in the present research, it has been compared with similar research. According to the differences in the optical setup and detection setup, only the trend of equivalence ratio with respect to change in OH*/CH* signal can be compared and the values of OH*/CH* signal will be unique for each specific optical setup and detection system. In order to validate the calibration curve, the work of Ikeda et.al [18] which has extracted the calibration curve for the same fuel (propane/air) has been chosen. The calibration curve Ikeda et.al. have extracted for Propane/air flame is shown in Figure 13. The trends in the present research and Ikeda et.al research are identical and both show the decrease in OH*/CH* signal by increase in the value of the equivalence ratio.

5 Conclusion

In this work, local chemiluminescence was implemented on a premixed laminar Propane/air bunsen burner flame. A Cassegrain-based optical system was developed to achieve high spatial resolution. The design process and optimization of the optical system were discussed. By the use of this optical system, chemiluminescent emissions of the OH* and CH* were measured from a control volume with a cylindrical effective volume. The cylinder is 58 micrometers in diameter and 3.4 millimeters in depth. The temporal resolution of the measurement system is 2 microseconds. The calibration curve between the OH*/CH* signal and the equivalence ratio was extracted for Propane/air flame and the developed measurement system. Using the developed Cassegrain-based optical system and optical filtering and detection system and the data acquisition system, finding the local equivalence ratio is possible for every propane/air flame with high temporal and spatial resolution.

References

[1] J. Kojima, Y. Ikeda, and T. Nakajima, "Basic Aspects of OH (A), CH (A), and C2 (d) Chemiluminescence in the Reaction Zone of Laminar Methane–air Premixed Flames," *Combustion and Flame,* Vol. 140, No. 1-2, pp. 34-45, 2005, doi: https://doi.org/10.1016/j.combustflame.2004.10.002.

[2] T. P. Clark, "Studies of OH, CO, CH, and C2 Radiation from Laminar and Turbulent Propane-Air and Ethylene-air Flames", *National Advisory Committee for Aeronautics Moffett Field*, CA, USA, Coporate: NASA Lewis Research Center, Cleveland, OH, Report: NACA TN 4266, June 1958, 23 p., https://firedoc.nist.gov/article/kXcxXYQBWEcjUZEYsQlv.

[3] H. N. Najm, P. H. Paul, C. J. Mueller, and P. S. Wyckoff, "On the Adequacy of Certain Experimental Observables as Measurements of Flame Burning Rate," *Combustion and Flame,* Vol. 113, No. 3, pp. 312-332, 1998, doi: https://doi.org/10.1016/S0010-2180(97)00209-5.

[4] B. Higgins, M. McQuay, F. Lacas, J.-C. Rolon, N. Darabiha, and S. Candel, "Systematic Measurements of OH Chemiluminescence for Fuel-lean, High-pressure, Premixed, Laminar Flames," *Fuel,* Vol. 80, No. 1, pp. 67-74, 2001, doi: https://doi.org/10.1016/S0016-2361(00)00069-7.

[5] A. Gaydon, and H. Wolfhard, "Spectroscopic Studies of Low-pressure Flames," in *Symposium on Combustion and Flame, and Explosion Phenomena*, 1948, Vol. 3, No. 1: Elsevier, pp. 504-518, doi: https://doi.org/10.1016/S1062-2896(49)80068-7.

[6] A. G. Gaydon, and H. Wolfhard, "Spectroscopic Studies of Low-pressure Flames. II. Effective Translational and Rotational Temperatures from CH Bands," *Proceedings of the Royal Society of London. Series A. Mathematical and Physical Sciences*, Vol. 199, No. 1056, pp. 89-104, 1949, doi: https://doi.org/10.1098/rspa.1949.0127.

[7] A. G. Gaydon, and H. Wolfhard, "Spectroscopic Studies of Low-pressure Flames IV. Measurements of Light Yield for C2 Bands," *Proceedings of the Royal Society of London. Series A. Mathematical and Physical Sciences*, Vol. 201, No. 1067, pp. 570-586, 1950, doi: https://doi.org/10.1098/rspa.1950.0079.

[8] F. Akamatsu, T. Wakabayashi, S. Tsushima, M. Katsuki, Y. Mizutani, Y. Ikeda, N. Kawahara, and T. Nakajima, "The Development of a Light-collecting Probe with High Spatial Resolution Applicable to Randomly Fluctuating Combustion Fields," *Measurement Science and Technology*, Vol. 10, No. 12, p. 1240, 1999, doi: 10.1088/0957-0233/10/12/316.

[9] Y. Ikeda, J. Kojima, and H. Hashimoto, "Local Chemiluminescence Spectra Measurements in a High-pressure Laminar Methane/Air Premixed Flame," *Proceedings of the Combustion Institute*, Vol. 29, No. 2, pp. 1495-1501, 2002, doi: https://doi.org/10.1016/S1540-7489(02)80183-3.

[10] Y. Hardalupas, M. Orain, C. S. Panoutsos, A.M.K.P. Taylor, J. Olofsson, H. Seyfried, M. Richter J. Hult, M. Aldén, F. Hermann, and J. Klingman, "Chemiluminescence Sensor for Local Equivalence Ratio of Reacting Mixtures of Fuel and Air (FLAMESEEK)," *Applied Thermal Engineering*, Vol. 24. 11-12, pp. 1619-1632, 2004, doi: https://doi.org/10.1016/j.applthermaleng.2003.10.028.

[11] Y. Hardalupas, C. Panoutsos, and A. Taylor, "Spatial Resolution of a Chemiluminescence Sensor for Local Heat-release Rate and Equivalence Ratio Measurements in a Model Gas Turbine Combustor," *Experiments in Fluids*, Vol. 49, pp. 883-909, 2010, doi: https://doi.org/10.1007/s00348-010-0915-z.

[12] T. Sugden, "Excited Species in Flames," *Annual Review of Physical Chemistry*, Vol. 13, No. 1, pp. 369-390, 1962, doi: https://doi.org/10.1146/annurev.pc.13.100162.002101.

[13] N. Docquier, F. Lacas, and S. Candel, "Closed-loop Equivalence Ratio Control of Premixed Combustors using Spectrally Resolved Chemiluminescence Measurements," *Proceedings of the Combustion Institute*, Vol. 29, No. 1, pp. 139-145, 2002, doi: https://doi.org/10.1016/S1540-7489(02)80022-0.

[14] P. J. Geddis, "Evaluation of Chemiluminescence as a Measurement Option for Industrial Flame Monitoring and Process Control", Degree: Master Thesis, OCLC Number: 1334672089, School of Graduate Studies – Theses, University of Toronto, Ontario, Canada (2009), https://tspace.library.utoronto.ca/bitstream/1807/18307/3/Geddis_Philip_J_200911_MASc_thesis.pdf.

[15] M. Lauer, and T. Sattelmayer, "On the Adequacy of Chemiluminescence as a Measure for Heat Release in Turbulent Flames with Mixture Gradients," *Journal of Engineering for Gas Turbines and Power*, Vol. 132, No. 6, pp. 061502 (8 pages), 2010, doi: https://doi.org/10.1115/1.4000126.

[16] M. Bass, C. DeCusatis, J. Enoch, V. Lakshminarayanan, G. Li, C. Macdonald, V. Mahajan, and E. V. Stryland, "*Handbook of Optics, Volume I: Geometrical and Physical Optics, Polarized Light, Components and Instruments(set)*", Third Edition, McGraw-Hill, Inc., New York, USA, 2009, ISBN:978-0-07-149889-0.

[17] M. Laikin, "*Lens Design, Third Edition*, Revised and Expanded", Third Edition, New York, NY: Marcel Dekker, Inc., USA, 2001, ISBN:0-8247-0507-6.

[18] Y. Ikeda, T. Kurahashi, N. Kawahara, and E. Tomita, "Temperature Measurements of Laminar Propane/Air Premixed Flame using Detailed OH* Spectra Intensity Ratio," in *12th International Symposium, Applications of Laser Techniques to Fluid Mechanics*, 2004, No. 1: Citeseer, pp. 1-11. [Online]. Available: https://citeseerx.ist.psu.edu/document?repid=rep1&type=pdf&doi=d4961c17b907245f716995db059f505ac0d88eda.

Nomenclature

English symbols

d	Deviation from ideal optical behavior
f	Focal length
MF	Merit function
n	Number of points
R	Radius of curvature
RMS	Root mean square
S	Distance between optical surface and the object or image
W	Weight of the deviation
x	x position of the point
y	y position of the point